Synthesis of intercalation compounds of molybdenum disulfide with nitrogen-containing organic molecules and study of their microstructure

A. S. Golub,[a]★ V. I. Zaikovskii,[b] N. D. Lenenko,[a] M. Danot,[c] and Yu. N. Novikov[a]

[a]*A. N. Nesmeyanov Institute of Organoelement Compounds, Russian Academy of Sciences, 28 ul. Vavilova, 119991 Moscow, Russian Federation. Fax: +7 (095) 135 5085. E-mail: golub@ineos.ac.ru*
[b]*G. K. Boreskov Institute of Catalysis, Siberian Branch of the Russian Academy of Sciences, 5 prosp. Akad. Lavrent´eva, 630090 Novosibirsk, Russian Federation. Fax: +7 (383 2) 34 3056. E-mail: viz@catalysis.nsk.su*
[c]*Institute of Materials Jean Rouxel, National Center for Scientific Research (CNRS), University of Nantes, 2 Rue de la Houssinière, BP 32229, 44332 Nantes, France.* Fax: +33 (0240) 37 3995. E-mail: danot@cnrs-imn.fr*

Reactions of single-layer dispersions of molybdenum disulfide with 2,2´-bipyridyl, *para*-phenylenediamine, and hexamethylenetetramine afford intercalation compounds consisting of alternating MoS_2 layers and layers formed by organic molecules. The structures of the intercalation compounds were characterized by X-ray powder diffraction and electron microscopy data. The influence of pH on the composition of resulting compounds and the packing of the intercalant was examined.

Key words: molybdenum disulfide, single-layer dispersions, intercalation compounds, electron microscopy.

Due to a layered-type structure,[1] molybdenum disulfide forms intercalation compounds, in which MoS_2 layers alternate with layers of organic compounds. Such intercalation compounds are of interest as lubricant components and potential ion conductors.[2,3] The electronic structure of MoS_2 (high energies of its acceptor levels) allows direct intercalation of this compound only with the use of strong reducing agents, such as alkali metals.[4] Recently, it has been demonstrated[5,6] that organic compounds can be introduced into space between the layers of molybdenum disulfide using single-layer dispersions of MoS_2.

A single-layer dispersion of MoS_2 prepared by hydration of $LiMoS_2$ is a ionic system consisting of negatively charged $(MoS_2)^{x-}$ layers, Li^+ cations, and hydroxide anions.[7]

$$LiMoS_2 \xrightarrow{H_2O} [Li^+ + (MoS_2)^{x-} + (1 - x)\,OH^-]_{aq} + + (1 - x)/2\,H_2$$

Due to the presence of a negative charge on the layers of dispersed molybdenum disulfide, it is possible to carry out ion-exchange reactions with particular water-soluble salts of quaternary alkylammonium cations (A^+), resulting in coagulation of the intercalation compounds A_xMoS_2.[6]

$$(MoS_2)^{x-} + A^+ \longrightarrow A_xMoS_2$$

Using phenanthroline (phen) as an example, it was demonstrated[8] that compounds, which can undergo protonation in an aqueous environment, can also be involved in reactions with single-layer dispersions of MoS_2 to form an intercalant layer as a mixture of cationic species and neutral molecules. The composition and structure of the $(phen)_xMoS_2$ compounds depend on pH of the environment.

It was of interest to study the reactions of single-layer dispersions of MoS_2 with nitrogen-containing compounds, which have a different ability to undergo protonation giving rise to mono- and dications in an aqueous-acidic environment, and to reveal the factors, which would allow one to control the structure of intercalation compounds as desired.

The aim of the present study was to examine intercalation of hexamethylenetetramine (hmta, $pK_a = 6.3$)[9], 2,2´-bipyridyl (bpy, $pK_{a_1} = 4.44$; $pK_{a_2} = -0.52$),[9] and *para*-phenylenediamine (ppda, $pK_{a_1} = 6.63$; $pK_{a_2} = 2.97$)[9] into molybdenum disulfide and determine the compositions and microstructures of the resulting layer compounds.

* Institut des Matériaux Jean Rouxel, CNRS-Université de Nantes, 2 Rue de la Houssinière, BP 32229, 44332 Nantes, France.

Published in Russian in *Izvestiya Akademii Nauk. Seriya Khimicheskaya,* No. 9, pp. 1837—1845, September, 2004.

1066-5285/04/5309-1914

Experimental

The $LiMoS_2$ compound was prepared by treating natural powdered MoS_2 (DM-1) with an excess of a 1.6 *M n*-butyllithium solution in hexane at 20 °C for one week followed by washing with hexane and vacuum drying. Then $LiMoS_2$ was dispersed in water (1 g L^{-1}) under argon with ultrasonic treatment.

Intercalation compounds were prepared by the addition of a hydrochloric acid solution (20 mL) containing hmta (analytical grade) (10 mol per mole of MoS_2), bpy (Aldrich), or ppda (analytical grade) (the amounts of the latter two compounds are given in Tables 1 and 2, respectively) to a dispersion of MoS_2 in water (100 mL) under vigorous stirring. After coagulation of the dispersion, the precipitate was filtered off, washed with water, and dried *in vacuo*. The pH of the reaction mixture was measured in the filtrate. The content of the intercalant (x) was determined from elemental analysis data (C, H, N, Mo, S). X-ray powder diffraction studies were carried out on DRON-3 and Siemens D5000 diffractometers (Cu-Kα radiation). The interlayer spacing (c) was determined from the positions of the 00l reflections. The thickness of the intercalant layer (Δc) was evaluated from the difference between the interlayer spacings for the intercalation compound and the starting MoS_2.

Studies by high-resolution transmission electron microscopy (HRTEM) and selected area electron diffraction (SAED) were performed on a JEM-2010 instrument (0.14 nm resolution, the accelerating voltage was 200 kV). Samples were dispersed on perforated carbon films supported on standard copper grids and then transferred to an electron microscope camera. The average interplanar spacings were determined from SAED images and using Fourier analysis of HRTEM images of periodic structures. The quality of the images were improved using Fourier filtration.

Results and Discussion

The reactions of aqueous hydrochloric acid solutions of hexamethylenetetramine (hmta), 2,2′-bipyridyl (bpy), and *para*-phenylenediamine (ppda) with dispersed MoS_2 produce black flocculent precipitates. A layer structure of the resulting compounds is evidenced by a set of 00l reflections in the X-ray diffraction patterns. As can be seen from Fig. 1, the introduction of an intercalant into the interlayer space leads to a shift of these reflections toward smaller 2θ angles, which is indicative of a substantial increase in the interlayer spacings (c) compared to those in the starting molybdenum disulfide (0.615 nm) or molybdenum disulfide precipitated from a single-layer dispersion in the absence of guest molecules (0.62 nm). According to elemental analysis data, the intercalation compounds thus prepared contain no noticeable amounts of chlorine, which confirms the ionic mechanism of their formation from the $(MoS_2)^{x-}$ macroanions and cationic forms of organic compounds and is consistent with the earlier data on the reactions of the salts R_4NX and phen · HCl with single-layer dispersions of MoS_2.[6,8]

Intercalation of 2,2′-bipyridyl

The addition of an equimolar amount of bpy in an HCl solution (the bpy : HCl molar ratio is 1) to a single-layer dispersion of molybdenum disulfide at pH 11.5 produces a precipitate of an intercalation compound, pH of

Table 1. Synthesis conditions, interlayer spacings (c), and thicknesses of the intercalant layer (Δc) in the $(bpy)_xMoS_2$ compounds

Sample	bpy : HCl : MoS_2 (mol. ratio)	pH	$bpyH^+$ (%)[a]	$bpyH^+$: MoS_2 (mol. ratio)	c	Δc
					nm	
1	1 : 1 : 1	5.7	5.2	0.052	0.97	0.35[c]
2	3 : 3 : 1	3.9	77.6	2.3	1.18	0.56
3	7 : 7 : 1	3.4	91.6	6.4	1.18	0.56
4	10 : 10 : 1	1.35	98.6[b]	9.9	0.97	0.35

[a] The equilibrium amount of $bpyH^+$ was calculated by the equation $\log(bpyH^+/bpy) = pK_a - pH$.
[b] The percentage of $bpyH_2^{2+}$ is 1.3%.
[c] Found (%): C, 10.60; H, 1.64; Mo, 50.27; N, 2.51; S, 32.62.

Table 2. Synthesis conditions, compositions, interlayer spacings (c), and thicknesses of the intercalant layer (Δc) in the $(ppda)_xMoS_2$ compounds

Sample	ppda : HCl : MoS_2 (mol. ratio)	pH	$ppdaH^+$	$ppdaH_2^{2+}$	Elemental composition (%)					x	c	Δc
			(%)		C	H	Mo	N	S		nm	
1	3 : 1 : 1	5.8	87.0	0.13	9.80	1.14	52.05	3.34	33.39	0.24	1.15	0.53
2	3 : 2 : 1	2.8	40.3	59.7	5.71	0.99	53.48	1.38	34.44	0.12	0.98	0.36
3	3 : 4 : 1	1.4	2.6	97.4	6.56	0.82	52.97	1.71	35.71	0.14	0.98	0.36

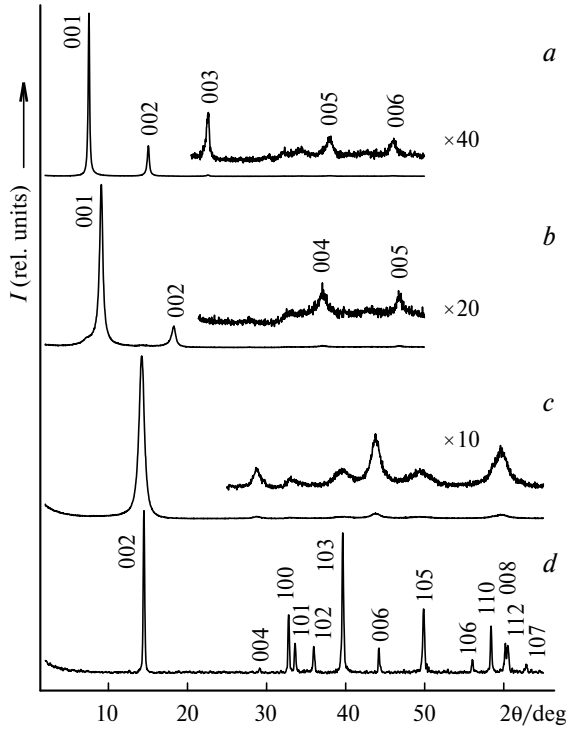

Fig. 1. X-ray diffraction patterns of the $(bpy)_xMoS_2$ intercalation compound freshly precipitated at pH 3.9 (*a*) and washed with water (*b*) and X-ray diffraction patterns of MoS_2 precipitated from a single-layer dispersion in the absence of an intercalant (*c*) and crystalline 2H-MoS_2 (*d*).

the final solution being 5.7 (see Table 1, sample *1*). According to the X-ray powder diffraction data, the intercalation compound obtained under these conditions is characterized by the interplanar spacing (*c*) of 0.97 nm, which corresponds to the 0.35 nm thickness of the intercalant layer (Δc). The latter parameter is equal to the van der Waals thickness of the aromatic rings, which indicates that the aromatic rings of bpy are parallel to the MoS_2 layers (Fig. 2, *a*). The bpy content of this compound determined experimentally (0.17 mol per mole of MoS_2) agrees well with the bpy content calculated for the orientation of bpy corresponding to the maximum close packing in the interlayer space (0.14 mol per mole of MoS_2).

The formation of intercalation compounds is initiated by the protonated form of a base, as has been demonstrated with phenanthroline.[8] At pH 5.7, the $bpyH^+$ monocation acts as this protonated form (see Table 1, sample *1*), the equilibrium concentration of which is 5.2% (under these conditions, the amount of $bpyH_2^{2+}$ is negligible). A low percentage of the protonated form suggests that not only cations but also neutral bpy molecules can be involved in the formation of the final compound. In both cases, the filled layer should be approximately the same thickness, because both forms of bpy have a planar structure.

An increase in the bpy : MoS_2 molar ratio to 3—7 leads to a decrease in pH of the final solution to 3.4—3.9. In this pH range, bpy occurs in solution predominantly in the monoprotonated form (78—92%, see Table 1, samples *2* and *3*), and the intercalant layer in the final compound consists predominantly of $bpyH^+$. Under these conditions, the intercalation compounds formed in the reaction mixture are characterized by a larger thickness of the intercalant layer (c = 1.18 nm, Δc = 0.56 nm). The observed increase in the interlayer spacing (as in compounds with phenanthroline[8]) is attributable to the positioning of bpy molecules perpendicular to the MoS_2 layers

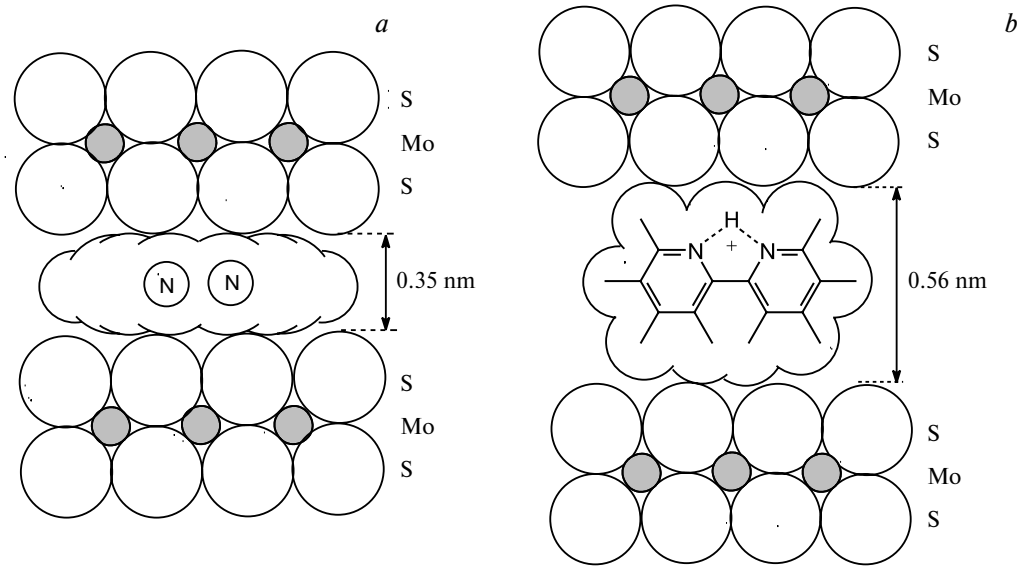

Fig. 2. Parallel (*a*) and perpendicular (*b*) orientations of the $bpyH^+$ cations relative to the matrix layers in MoS_2 compounds intercalated with bipyridyl.

(see Fig. 2, *b*). However, attempts to isolate these compounds by washing failed because this treatment, unlike treatment of MoS_2 intercalated with phenanthroline, was accompanied by a gradual decrease in the *c* parameter. Within a few hours, the *c* parameter became as small as 0.97—0.98 nm, which is characteristic of compounds with a parallel orientation of bpy molecules. The compositions of the washed samples ($x = 0.17$) also correspond to this type of compounds.

The difference in stability of MoS_2 compounds intercalated with bpy and phen can be explained in terms of the structural features of these heterocycles. Actually, exposure of MoS_2 intercalated with bpy or phen to water is, apparently, accompanied by a gradual decrease in the negative charge on the MoS_2 layers due to redox reactions of the $(MoS_2)^{x-}$ macroanions with water molecules.[7]

This should lead to simultaneous deprotonation of the organic cations in the interlayer space. In the case of $phenH^+$, the molecular geometry remains unchanged upon deprotonation. In the $bpyH^+$ cations, the nitrogen atoms are in *cis* positions relative to the C(1)—C(1´) bond, whereas the *trans* configuration is typical of the neutral bpy molecules.[10,11] Hence, deprotonation of $bpyH^+$ should be accompanied by rotation of each aromatic ring of the bpy molecule about the C(1)—C(1´) bond by 90° in opposite directions (Fig. 3), resulting in the parallel orientation of the bpy molecules relative to the MoS_2 layers. This change in the orientation should decrease the number of bpy molecules due to their displacement from the interlayer space, because each bpy molecule located parallel to the layer occupies a larger area on the MoS_2 layer compared to the molecular area occupied by the $bpyH^+$ cation in the orientation shown in Fig. 2, *b*.

The negative charge of the MoS_2 layers decreases not only upon treatment of the final compound with water but also at the step of formation of the intercalation compound in single-layer dispersions. This is associated with the fact that the reaction proceeds in an acidic environment, and removal of the negative charge from the $(MoS_2)^{x-}$ layers is substantially accelerated with decreasing pH.[8,12] The ratio between the rate of formation of the intercalation compound and the rate of removal of the charges from the $(MoS_2)^{x-}$ layers evidently determines the composition and structure of the final compounds, all other factors being the same. At pH 3.4 and 3.9 (77.6 and 91.6% of $bpyH^+$, respectively; see Table 1, samples *2* and *3*), the rate of formation of the final compound is, apparently, higher than the rate of removal of the charge from the $(MoS_2)^{x-}$ layers. Hence, the $(MoS_2)^{x-}$ layers bear a fairly high negative charge upon precipitation of the final compound. The corresponding amount of the $bpyH^+$ counterions in the interlayer space is required to neutralize the charge. This is possible only if these cations are oriented perpendicular to the MoS_2 layers. To the contrary, at pH 1.35 (98.6% of $bpyH^+$, see Table 1, sample *4*), the rate of removal of the charges from the $(MoS_2)^{x-}$ layers is, apparently, higher than the rate of formation of the final compound, resulting in the formation of a compound in which the $bpyH^+$ cations are parallel to the MoS_2 layers ($c = 0.98$ nm). It could also be imagined that the $bpyH_2^{2+}$ dications are involved in the formation of a layered compound, because this could compensate the negative charge of the MoS_2 layers with a smaller amount of cations. However, this explanation seems to be less probable, because the concentration of the dications is two orders of magnitude lower than the concentration of the $bpyH^+$ monocations. Finally, the formation of a compound, in which the MoS_2 layers are arranged parallel to $bpyH^+$, at pH 5.7 (see Table 1, sample *1*) is favored by a low concentration of the cationic form in the solution (5.2%), which retards the formation of the intercalation compound.

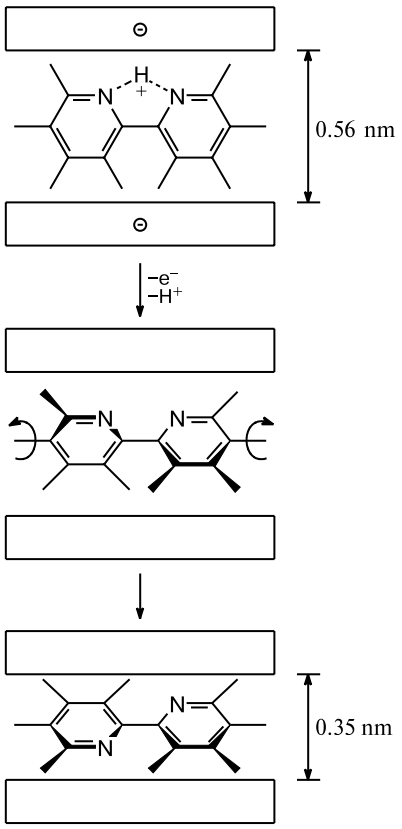

Fig. 3. Hypothetical scheme of the transformation of the intercalation compound $(bpy)_xMoS_2$ ($c = 1.18$ nm) upon deprotonation of the bipyridylium cations in the interlayer space.

Intercalation of para-phenylenediamine

Let us consider the differences in the behavior of bpy and ppda associated with the differences in the basicity of these compounds. Taking into account the higher basicity of ppda compared to bpy, one would expect the presence

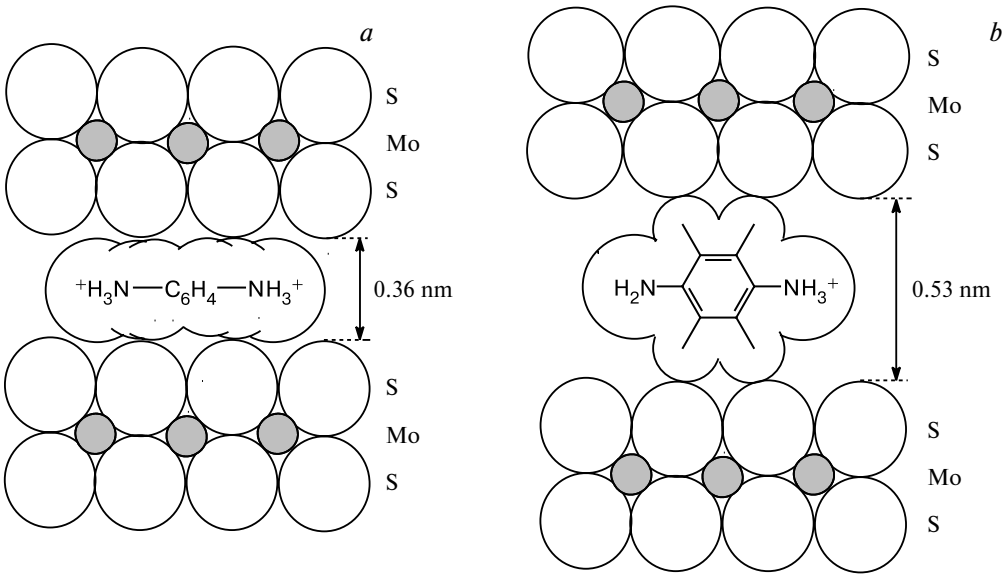

Fig. 4. Parallel (*a*) and perpendicular (*b*) orientations of the aromatic rings of ppda relative to the matrix layers in MoS_2 compounds intercalated with *para*-phenylenediamine.

of the monoprotonated form of bpy in substantial concentrations in solutions at higher pH. In addition, moderately acidic media can contain the $ppdaH_2^{2+}$ dications in high concentrations due to thier fairly high pK_{a_2}, and these dications can be involved in the formation of intercalation compounds.

At pH 5.8 (see Table 2, sample *1*), the percentage of $ppdaH^+$ in solution is 87%. In this case, the resulting compound is characterized by the maximum content of intercalated ppda ($x = 0.24$). In this compound, the thickness of the layer filled with the intercalant ($\Delta c = 0.53$ nm) suggests the nearly perpendicular arrangement of the aromatic rings of ppda relative to the MoS_2 layers (Fig. 4, *b*). The organic cations are closely packed in the interlayer space, as evidenced by the fact that the experimental composition is similar to that calculated for the close packing using this model ($x = 0.25$). A comparison of the data for samples *1* (see Tables 1 and 2) confirms the above suggestion that the composition and structure of the compound with bpy formed in this pH range are determined by a low concentration of $bpyH^+$ in solution.

A decrease in pH to 2.8 and 1.4 (see Table 2, samples *2* and *3*) results in the formation of compounds with a lower content of ppda ($x = 0.12$—0.14). According to the X-ray powder diffraction data ($\Delta c = 0.36$ nm), the ppda molecules are located parallel to the MoS_2 layers (Fig. 4, *a*). As can be seen from Table 2, under these conditions the $ppdaH_2^{2+}$ dications account for 59.7 and 97.4%, respectively, of ppda present in the reaction mixture. Presumably, the composition and structure of the final compounds are determined by incorporation of these species, because the negative charge of the $(MoS_2)^{x-}$ layers is compensated by half as smaller amount of the dications as that of the $ppdaH^+$ monocations. This compensation can take place in the case of the parallel orientation of the $ppdaH_2^{2+}$ molecules relative to the MoS_2 layers. This is also confirmed by comparing the data for samples *3* (see Table 1) and *2* (see Table 2). In both cases, the solutions have similar pH (3.4 and 2.8, respectively). Consequently, the rates of discharge of the $(MoS_2)^{x-}$ layers are also similar. However, the bpy molecules in the compound formed in the first case are located perpendicular to the $(MoS_2)^{x-}$ layers, because the solution contains predominantly the monocations (91.6%). At the same time, the ppda molecules are located parallel to the $(MoS_2)^{x-}$ layers in the compound formed in the second case, because the ppda molecules occur in solution predominantly in the dicationic form (59.7%).

Intercalation of hexamethylenetetramine

The hmta molecules, like ppda, possess a fairly high basicity. However, only the $hmtaH^+$ monocation is a stable protonated form, whereas the addition of the second proton initiates hydrolysis of hmta.[13] The equilibrium concentrations of $hmtaH^+$ (~50%) are high already in neutral and weakly acidic environment, which is favorable for initiation of precipitation of intercalation compounds from single-layer dispersions. At pH 2.3—7.5, the formation of particles of intercalation compounds in single-layer dispersions is observed virtually immediately after the addition of hmta. The formation of the compounds in an alkaline medium occurs more slowly. At pH 11.5, it is necessary to keep single-layer solutions overnight for their clarification. The structural parameters of hmta, unlike those of ppda and bpy, are independent of pH. All

compounds have the composition $(hmta)_xMoS_2$ with $x = 0.22—0.25$ and the interlayer distance $c = 1.16$ nm. The fact that the structural parameters remain unchanged is attributable to a nearly spherical shape of the hmta molecule. The experimental composition corresponds to a close packing of the hmta molecules with a van der Waals diameter of 0.5—0.6 nm in a monolayer between the layers of molybdenum disulfide.

Microstructure of compounds prepared from single-layer dispersions as evidenced by electron microscopy data

The characteristic features of the morphology and microstructure of the intercalation compounds prepared from single-layer dispersions are most clearly seen in comparison with the starting natural crystalline molybdenum disulfide (2H-MoS_2). In the crystals of this most stable hexagonal modification of molybdenum disulfide, the sulfur layers alternate in the AA BB sequence to form trigonal prisms within each such fragment (AA and BB).[1] The centers of the prisms are occupied by Mo atoms. The layer structure is pronounced in the side projections of the particles, where periodic contrast is observed (Fig. 5, *a*). The repetition period determined from these images ($d = 0.615$ nm) is equal to the interlayer spacing in 2H-MoS_2. In addition, the periodic contrast along the layers is observed in the [110] projection as short strokes perpendicular to the layer (Fig. 5, *b*). In appearance and orientation, these strokes are consistent with the image simulated for this projection of this structure (Fig. 5, *c*) using the available structural data (space group $P6_3/mmc$, $a = 0.316$ nm, $c = 2 \cdot 0.615$ nm),[14] and the periodicity of the strokes corresponds to the interplanar distance $d_{100} = 0.274$ nm for 2H-MoS_2.

Morphology of layers of intercalation compounds. In the absence of an intercalant, molybdenum disulfide precipitates from a single-layer dispersion as particles, whose shape, although remaining platelet (as in crystalline 2H-MoS_2), is characterized by a larger number of distortions and faults (Fig. 6). Most of particles are several nanometers thick, but very thin particles consisting of one or a few layers of molybdenum disulfide are also observed (see Fig. 6, *a*). The interlayer distance determined from the images of particles of precipitated nonintercalated MoS_2 is approximately equal to 0.62 nm, which is similar

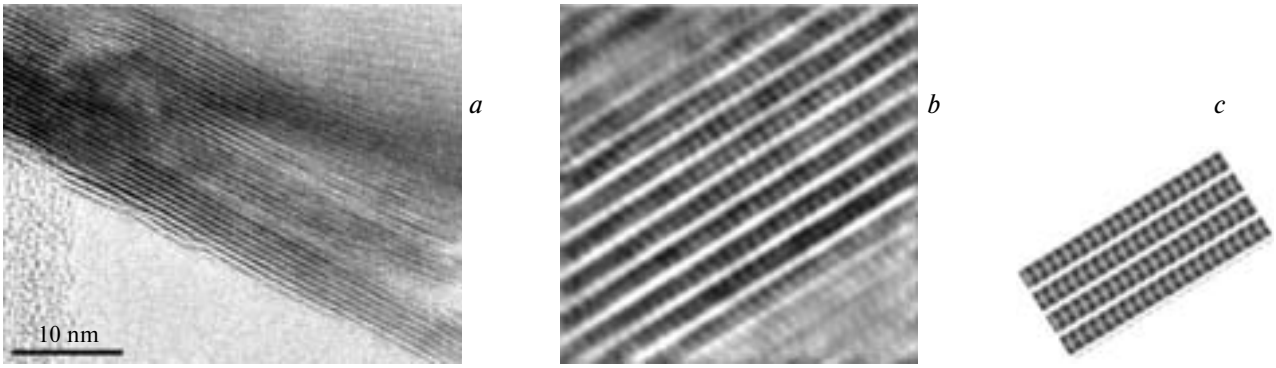

Fig. 5. The HRTEM images of crystalline 2H-MoS_2: the layered structure of crystallites with an interlayer distance of 0.615 nm (*a*), periodic contrast along the MoS_2 layers (*b*), the calculated image projected onto the [110] plane (*c*).

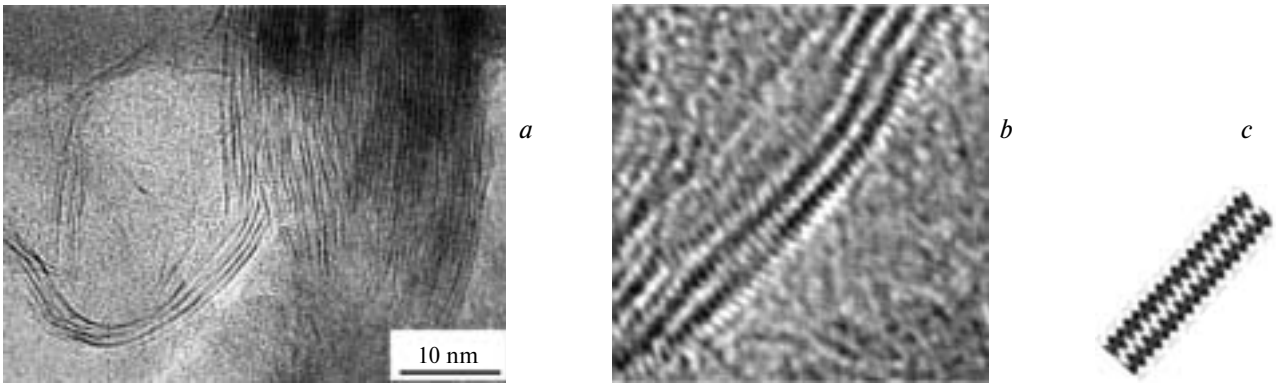

Fig. 6. The HRTEM images of MoS_2 precipitated from a single-layer dispersion: the structure of particles with an interlayer spacing of 0.62 nm (*a*), periodic contrast along the MoS_2 layers (*b*), the calculated image for the MoS_2 layers with a diamond-chain superstructure[21] projected onto the [110] plane (*c*).

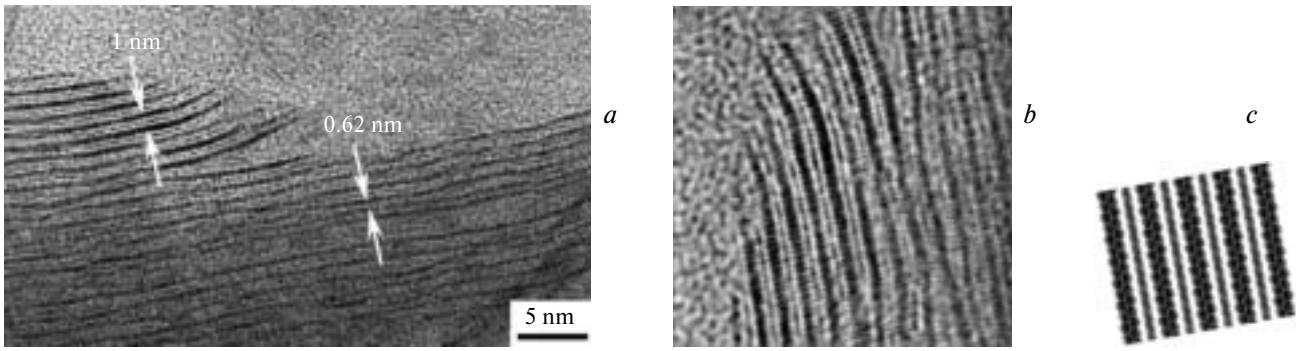

Fig. 7. The HRTEM images of $(bpy)_{0.17}MoS_2$: the intercalated structure (different distances between the MoS_2 layers are indicated by arrows) (*a*), periodic contrast along the MoS_2 and bpy layers (*b*), the calculated image projected onto the [110] plane (*c*).

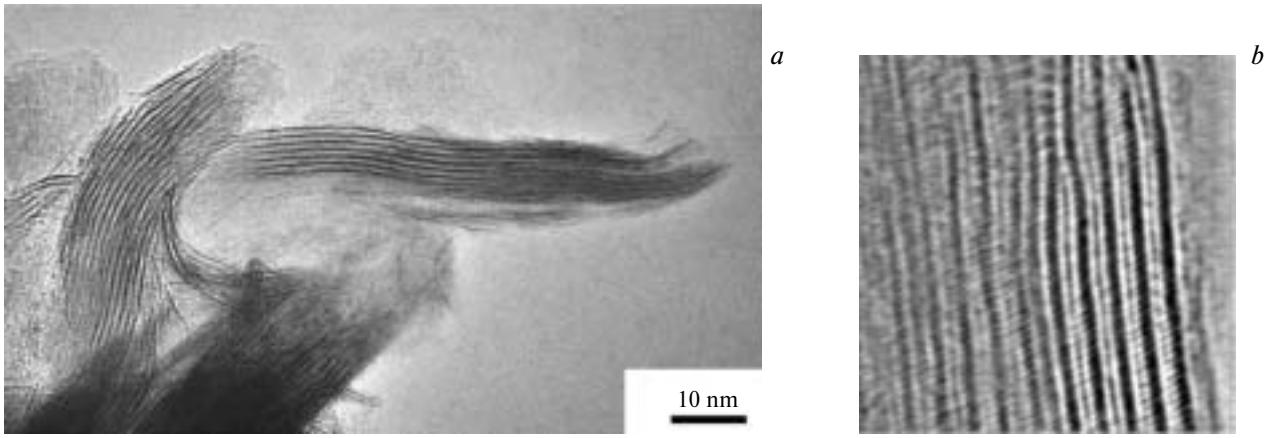

Fig. 8. The HRTEM images of $(hmta)_{0.2}MoS_2$: the intercalated structure with an interlayer spacing of 1.1 nm (*a*), contrast along the layers (*b*).

to the corresponding distance for 2H-MoS_2. The regularly arranged MoS_2 layers are observed also in the images of particles of the compounds intercalated with bpy and hmta. However, these images have an additional band between the layers associated with the presence of a molecular layer of the guest (Figs 7, *a*, *b* and 8, *a*, *b*). The average periodicity in the arrangement of the layers is 1.0 and 1.1 nm for $(bpy)_{0.17}MoS_2$ and $(hmta)_{0.2}MoS_2$, respectively, which is in satisfactory agreement with the parameters determined by X-ray powder diffraction. In addition, the side projections show that the MoS_2 layers are strongly fragmented after dispersion. The length of the fragments along the layer is ~10—50 nm. The fragments involved in the particles consisting of a small number of layers show a tendency toward a nonlinear morphology. The superposition of the layers is characterized by a large amount of dislocations, resulting in the disruption of a regular packing characteristic of the starting molybdenum disulfide. In periodic layer structures of intercalation compounds, there are, in addition, irregularities in the interlayer distances due to variations in the thickness of the layer filled with the guest molecules or the existence of unfilled interlayer spaces. For example, the images of the particles of the compound with bipyridyl (see Fig. 7, *a*) show bands spaced at ~1 nm, which corresponds to the parallel orientation of the planes of the bipyridyl molecules relative to the layers. In addition, there are bands located both at longer and shorter distances (0.62 nm). The distances larger than 1 nm are indicative of a deviation of the molecules from the parallel orientation, whereas shorter distances are indicative of the absence of the molecules in this interlayer space. For the compound with hmta, whose molecules are more isotropic in shape, the irregularities in the interlayer distances are less pronounced (see Fig. 8).

Structure of layers of molybdenum disulfide in intercalation compounds. For dispersed materials, the images of the [110] side projections of the particles show a zigzag contrast in the direction along the layers (see Figs 6, *b* and 7, *b*). This feature is characteristic not only of the intercalation compounds but also of nonintercalated MoS_2 (see Fig. 6, *b*), which indicates that the structure of the MoS_2 layers changes in the course of dispersion and this change is retained in the final compounds. This conclusion is consistent with the results of investigations of materials, which were precipitated from single-layer disper-

sions of MoS_2, by X-ray powder diffraction,[15] Raman spectroscopy,[16] and EXAFS spectroscopy.[17—19] The transformations of the atomic structure of molybdenum disulfide are generally associated with the charge transfer to its layers upon intercalation of lithium. The compound with the latter, *viz.*, $LiMoS_2$, serves as a precursor for the preparation of dispersions. The precise atomic structures of neither $LiMoS_2$ nor its dispersion products were determined. The octahedral coordination environment of molybdenum by sulfur is common to all structural models of these compounds discussed in the literature. This coordination environment occurs instead of the trigonal-prismatic environment characteristic of the 2H-MoS_2 structure (for more details, see Ref. 20). According to the extended X-ray absorption fine structure data, the regular Mo...Mo distances (0.316 nm) in the layer of 2H-MoS_2 change to a set of nonequivalent distances (involving the direct Mo—Mo bonds) in materials prepared from dispersions. Based on these data, various modes of ordering of the molybdenum atoms in the layer were proposed (Fig. 9).

The observed contrast of the layers of precipitated nonintercalated MoS_2 (see Fig. 6, *b*) is best consistent with the contrast simulated (see Fig. 6, *c*) with the use of the model proposed recently and based on the results of calculations.[21] In this model, the molybdenum atoms in the layer form a diamond-chain structure (see Fig. 9, *c*). In the cited study, the structure was described as triclinic with retention of the axes of the basic lattice (space group $P\bar{1}$, $a = b$, $\alpha = \beta = 90°$, $\gamma = 120°$). The images of intercalation compounds, in particular, of $(bpy)_{0.17}MoS_2$, calculated using this model of ordering of molybdenum atoms (see Fig. 7, *b*, *c*; the structure with a parallel arrangement of the bpy molecules relative to the layers was simulated), are also in good agreement with experimental data.

The differences in the structures of the S—Mo—S layers in the compounds prepared from dispersions and 2H-MoS_2 were revealed in studies by electron microdiffraction in the direction perpendicular to the layers (Fig. 10). In the diffraction patterns of the precipitated compounds, the {*hk*0} reflections are highly diffuse. This is, apparently, associated with the fact the structures of the materials are poorly ordered. In addition, the diffraction patterns of the compounds precipitated from dispersions contain not only main reflections characteristic of the hexagonal lattice of 2H-MoS_2 but also additional reflections, whose intensities increase in the series $MoS_2 < (bpy)_{0.17}MoS_2 < (hmta)_{0.2}MoS_2$. These reflections are also indexed in the hexagonal system. However, the parameter $a_1 \approx 0.63$ nm of the lattice corresponding to these reflections is twice as large as that of the 2H-MoS_2 lattice ($a = 0.316$ nm). Analogous extra reflections have been observed earlier in the electron diffraction patterns for precipitated MoS_2 [22,23] and Cu_xMoS_2.[24]

The presence of such reflections is consistent with the appearance of superstructure ordering in particles of precipitated materials due to clusterization of molybdenum atoms in the layers. However, a comparison of the experimental patterns of distortions of the charged MoS_2 layer (see Fig. 10, *b—d*) with the pattern calculated for the optimized model[21] (see Fig. 10, *e*) shows that, although the extra reflections in these patterns are similar in positions, the reflections of the same order are substantially different in intensities. The reason is that the symmetry of the basic hexagonal layer is lowered considering the presence of the diamond chains (see Fig. 9, *c*). The symmetrical character of the extra reflections in the experimental patterns is attributable to overlapping of reflections from similar structures with orientations following a certain law (twinning phenomenon). The observed diffraction pattern, involving averaging of the intensities of the extra reflections, can occur due to superposition of the reflections from three fragments, which are rotated around the [001] direction by 120° relative to two other fragments (see Fig. 10, *f*). The existence of a set of structures is indirectly confirmed by the presence of a pronounced azimuthal distortion of reflections, which appears due to disorder of the orientations of superstructures about the [001] direction. Earlier,[22,23] it has been hypothesized that twinning occurs due to superposition of the adjacent layers of nonintercalated MoS_2 precipitated from disper-

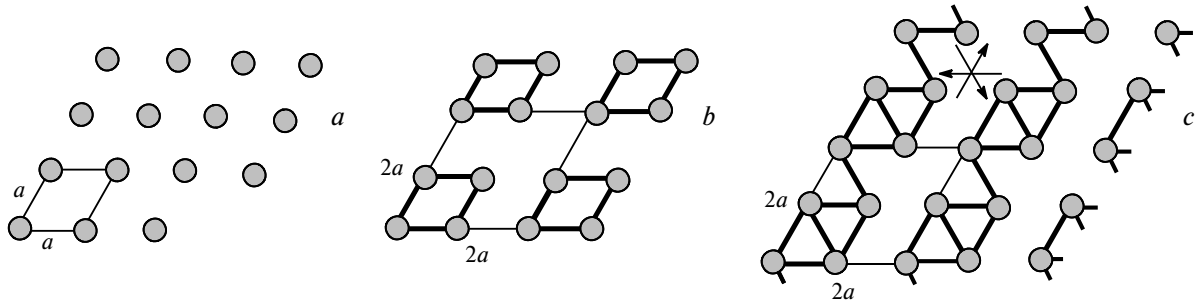

Fig. 9. Arrangement of molybdenum atoms in the *ab* plane of the hexagonal unit cell $a \times a$ (*a*) and models of the formation of tetrameric (*b*) and diamond-chain (*c*) superstructures $2a \times 2a$. The possible directions of the chains in the basic structure are indicated by arrows.

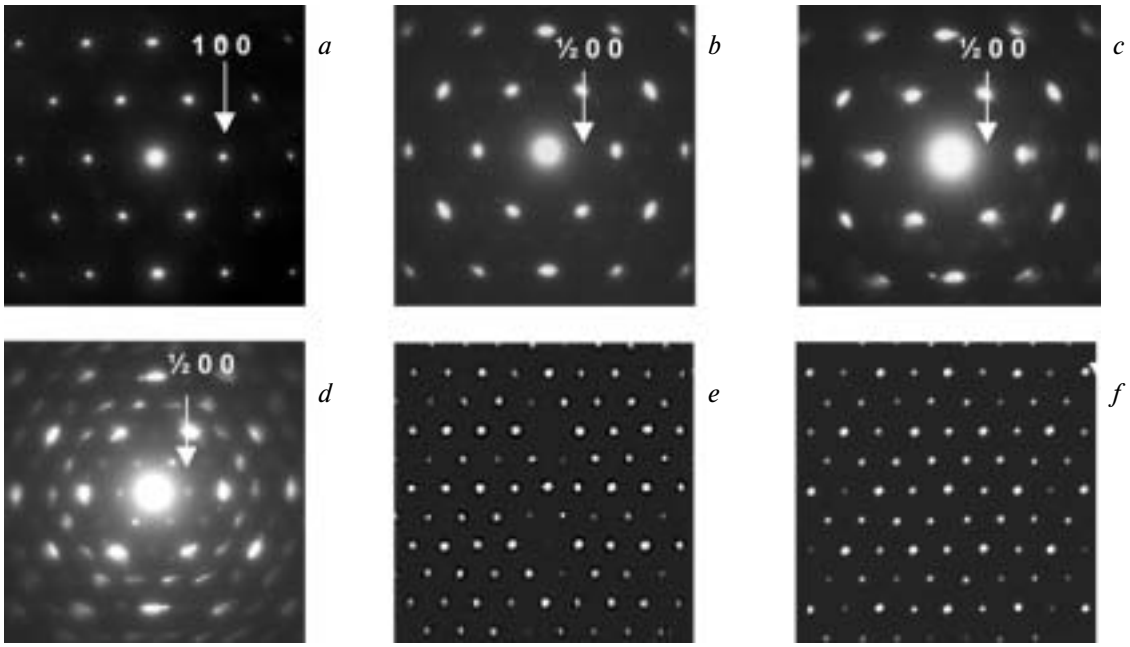

Fig. 10. Diffraction patterns of the [001] projections of samples of 2H-MoS_2 (*a*), MoS_2 from a dispersion (*b*), $(bpy)_{0.17}MoS_2$ (*c*), and $(hmta)_{0.2}MoS_2$ (*d*) and calculated diffraction patterns for a diamond-chain model of distortions of the MoS_2 layer (*e*) and the superposition of three such structures with a rotation angle of 120° (*f*). The positions of the basic 100 reflections and superstructure ½00 reflections are indicated by arrows.

sions. However, the correlations in the superposition of the layers are contradictory to the absence of the *h*0*l* lines in the X-ray powder diffraction patterns. At the same time, the diffuse character of reflections in electron diffraction patterns indicates that the sizes of ordered regions are substantially smaller that the diameter of the electron beam (100—200 nm). Hence, the region under study can contain a set of superstructurally ordered fragments of one layer. The angle of 120° is characteristic of the mutual orientation of the ordered regions formed within one layer, because the basic hexagonal layer with a periodicity of $a \times a$ has six directions for the occurrence of the chains, three of which are nonequivalent (see Fig. 9, *c*). A superposition of these layers with a rotation about the [001] directions also provides conditions for consistent diffraction but only in 60° intervals. However, the regular superposition of the MoS_2 monolayers in the intercalation compounds with organic guests, which are incommensurate with the lattice of the sulfide layer, is unlikely. The electron diffraction patterns are most likely to be associated with the presence of a set of ordered fragments within each layer.

* * *

Investigation of intercalation of bipyridyl, *para*-phenylenediamine, and hexamethylenetetramine into molybdenum disulfide with the use of single-layer dispersions of MoS_2 demonstrated that this process is described by an ionic model of the structure of these dispersions.

Depending on the pH of the reaction medium, bipyridyl and *para*-phenylenediamine form two types of intercalation compounds with molybdenum disulfide with characteristic composition and thickness of organic monolayers.

According to electron microscopy data, the particles of the compounds under study contain from several to several tens of monolayers of molybdenum disulfide alternating with the guest layers. The MoS_2 monolayers in particles consist of fragments with sizes of 10—50 nm along the layer. The formation of single-layer dispersions leads to a change in the interlayer atomic structure of molybdenum disulfide. The results obtained in the present study are consistent with the calculation model, which includes the octahedral environment of molybdenum by sulfur and superstructure ordering of molybdenum atoms to form diamond-chain structures.

This study was financially supported by the Russian Academy of Sciences (the Programs "Fundamental Problems of Physics and Chemistry of Nano-sized Systems and Nanomaterials" and "Scientific Fundamentals of Chemical Technologies and Preparation of Pilot Batches of Substances and Materials").

References

1. G. V. Subba Rao and M. W. Shafer, in *Intercalated Layered Materials*, D. Riedel Publ. Co, Holland, 1979, 99.

2. L. N. Sentyurikhina and E. M. Oparina, *Tverdye disul´fid-molibdenovye smazki* [*Solid Molybdenum Disulfide Lubricants*], Khimiya, Moscow, 1966, 152 pp. (in Russian).
3. A. P. Krasnov, O. V. Afonicheva, V. A. Mit´, A. S. Golub´, I. B. Shumilova, and Yu. N. Novikov, *Trenie Iznos*, 1996, **17**, 799 [*J. Frict. Wear*, 1996, **17** (Engl. Transl.)].
4. R. H. Friend and A. D. Yoffe, *Adv. Phys.*, 1987, **36**, 1.
5. W. M. R. Divigalpitiya, R. F. Frindt, and S. R. Morrison, *Science*, 1989, **246**, 4928.
6. A. S. Golub´, G. A. Protsenko, L. V. Gumileva, A. G. Buyanovskaya, and Yu. N. Novikov, *Izv. Akad. Nauk, Ser. Khim.*, 1993, 672 [*Russ. Chem. Bull.*, 1993, **42**, 632 (Engl. Transl.)].
7. M. Danot, J. L. Mansot, A. S. Golub, G. A. Protzenko, P. B. Fabritchnyi, Yu. N. Novikov, and J. Rouxel, *Mat. Res. Bull.*, 1994, **29**, 833.
8. A. S. Golub, I. B. Shumilova, Yu. N. Novikov, J. L. Mansot, and M. Danot, *Solid State Ionics*, 1996, **91**, 307.
9. D. D. Perrin, *Dissociation Constants of Organic Bases in Aqueous Solution*, Butterworths, London, 1965, 473 pp.
10. A. Parlow and H. Hartl, *Z. Naturforsch., Teil B*, 1985, **40**, 45.
11. L. L. Merritt and E. D. Schroeder, *Acta Crystallogr.*, 1956, **9**, 801.
12. B. K. Miremadi, T. Cowan, and S. R. Morrisson, *J. Appl. Phys.*, 1991, **69**, 6373.
13. H. Tada, *J. Am. Chem. Soc.*, 1960, **82**, 255.
14. R. G. Dickinson and L. Pauling, *J. Am. Chem. Soc.*, 1923, **45**, 1466.
15. Y. V. Zubavichus, A. S. Golub, N. D. Lenenko, Yu. L. Slovokhotov, Yu. N. Novikov, and M. Danot, *Mat. Res. Bull.*, 1999, **34**, 1601.
16. D. Yang, S. Jiménez-Sandoval, W. M. R. Divigalpitiya, J. C. Irwin, and R. F. Frind, *Phys. Rev. B*, 1991, **43**, 12053.
17. P. Joensen, E. D. Crozier, N. Alberding, and R. F. Frindt, *J. Phys. C*, 1987, **20**, 4043.
18. K. E. Dungey, M. D. Curtis, and J. E. Penner-Hahn, *J. Catal.*, 1998, **175**, 129.
19. Y. V. Zubavichus, A. S. Golub, Yu. N. Novikov, Yu. L. Slovokhotov, P. J. Schilling, and R. C. Tittsworth, *J. Phys. IV France*, 1997, **7**, *Colloque C2*, 1057.
20. A. S. Golub´, Ya. V. Zubavichus, Yu. L. Slovokhotov, and Yu. N. Novikov, *Usp. Khim.*, 2003, **72**, 138 [*Russ. Chem. Rev.*, 2003, **72**, 123 (Engl. Transl.)].
21. X. Rocquefelte, F. Boucher, P. Gressier, and G. Ouvrard, *Phys. Rev. B*, 2000, **62**, 2397.
22. X. R. Qin, D. Yang, R. F. Frindt, and J. C. Irwin, *Ultramicroscopy*, 1992, **42—44**, 630.
23. J. Heising and M. G. Kanatzidis, *J. Am. Chem. Soc.*, 1999, **121**, 638.
24. A. S. Golub, I. B. Shumilova, Y. V. Zubavichus, Yu. L. Slovokhotov, Yu. N. Novikov, A. M. Marie, and M. Danot, *Solid State Ionics*, 1999, **122**, 137.

Received April 30, 2004;
in revised form June 25, 2004